Synthesis, Structural Characterisation, and Cytotoxicity Studies of Bi, W, and Mo containing Homo- and Hetero-bimetallic Polyoxometalates

Senevirathna, D.; Werrett, M.; Kubeil, M.; Stephan, H.; Andrews, P.;

Originally published:

October 2019

Dalton Transactions 48(2019), 15962-15969

DOI: https://doi.org/10.1039/C9DT03288F

Synthesis, Structural Characterisation, and Cytotoxicity Studies of Bi, W, and Mo containing Homo- and Hetero-bimetallic Polyoxometalates

Dimuthu C. Senevirathna,[a] Melissa. V. Werrett,[a] Manja Kubeil, [b] Holger Stephan,[b] and Philip C. Andrews[a*]

[a]School of Chemistry, Monash University, Clayton, Melbourne, VIC 3800, Australia.
Email: phil.andrews@monash.edu
[b]Institute of Radiopharmaceutical Cancer Research, Helmholtz-Zentrum Dresden-Rossendorf, Bautzner Landstraße 400, D-01328 Dresden, Germany

Electronic supplementary information (ESI) available. CCDC numbers 1916373-1916375. For ESI and crystallographic data in CIF or other electronic format see DOI: ____.

Abstract

Three new and different homo- and hetero-bimetallic polyoxometalate (POM) species have been synthesised by simple one-pot synthetic methods utilising naturally occurring bismite (Bi_2O_3) (or $Bi(NO_3)_3{\cdot}5H_2O$) and aryl sulfonic acids. The POM species isolated are $\{(NH_4)_{14}[Bi_2W_{22}O_{76}]{\cdot}14H_2O\}$ (**1**$\cdot 14H_2O$), $\{NH_4[Bi(DMSO)_7][Mo_8O_{26}]{\cdot}H_2O\}$ (**2**$\cdot H_2O$) and $\{[(NH_4)_4(Mo_{36}O_{108}(OH)_4{\cdot}16H_2O)]{\cdot}45H_2O\}$ (**3**$\cdot 45H_2O$). The compounds have been characterised by X-ray crystallography, energy dispersive X-ray spectroscopy (EDX), powdered X-ray diffraction (PXRD), mass spectrometry (ESI-MS), Raman spectroscopy, thermogravimetric (TGA) and ICP analyis. *In vitro* cytoxicity and proliferation studies conducted on **1** and **3**, highlight the low toxicity of these species.

Introduction

Polyoxometalates (POMs) have attracted significant interest in the last few decades due to their fascinating structural diversity and potential applications in many areas, including biomedicine, catalysis and materials science.[1–9] Specifically, their favourable solubility and stability in aqueous environments and biological systems has seen POMs gain further interest in pharmaceutical applications in recent years.[10–17] It has been reported that POMs and their inorganic-organic hybrids have shown antibacterial, antidiabetic, antiprotozoal, antiproliferative, and antiviral activity.[1,18–27 28,29] An effective anti-tumor activity is obtained in particular for transition metal-containing and redox-active POMs and is mostly based on cell apoptosis. Due to a strong interaction of these polyanions with cell surfaces, POMs can selectively block certain enzymes[30–35] and can be utilised as protein-hydrolysing agents. The utilisation of high atomic number (Z) containing clusters (W, Ta, Gd, Re, Bi) as X-ray contrast agents in CT imaging[36] and in the emerging field of radiosensitisers in cancer therapy, is driving some of the recent research into the design and synthesis of high nuclearity POMs.[37–39] Very recently, a well-defined polyoxotungstate has been discovered to act as an effective radiosensitiser.[10] POMs offer a way to potentially deliver a high payload of metal(s) into the body for those applications. The highly dense nature of the clusters provides a way to incorporate multiple metal sites with these hetero-bimetallic POMs having the potential to be utilised for multimodal applications.

In particular, bismuth has a reputation of exhibiting low toxicity compared to other high atomic number p-block elements possessing lone pairs, such as Sn, Pb, As, and Sb.[40,41] This makes bismuth an attractive metal to incorporate into POMs for applications in medicine. Bismuth heteropolytungstate (BiP_5W_{30}) nanoclusters have been reported as radiosensitisers for the tumor microenvironment-manipulated enhancement of radiotherapy.[42] Furthermore, Krebs-type tungstobismuthates, i.e., $[(W(OH)_2)_2(Mn(H_2O)_3)_2(Na_3(H_2O)_{14})(BiW_9O_{33})_2](Himi)_2{\cdot}16H_2O$ (imi=iminazole) are able to increase the expression of p53 (transcription factor that induces anti-carcinogenesis events) activating apoptosis leading to cell growth arrest and inhibition of angiogenesis. .[43,44] Despite this, compared to many other heteroatoms (Co, Mn and As)[45,46] there are only a small number of reports of POMs containing Bi^{3+}, which has been attributed to the difficult synthesis, due to lone pairs and the large ionic radii of Bi^{3+}.[47]

The general synthesis of Bi containing clusters had been investigated utilising a range of ligands systems and reaction conditions,[48,49] however it is well documented that their controlled synthesis still poses a challenge.[50,51] We recently reported the synthesis of a series of bismuth-oxido sulfonato clusters, polymers and ion pairs utilising mineral bismuthinite (Bi_2O_3) from a series of aryl sulfonic acids, in an attempt to

systematically understand and control cluster formation.[52] While some trends were evident there was still ambiguity in controlling the size and nuclearity of the final systems. Many POM systems exhibit high stability, appropriate aqueous solubility and biocompatibility as well as potential for functionalisation. On the way to developing non-toxic cluster compounds, we wanted to investigate the synthesis of Bi-containing POMs with incorporated W or Mo for potential applications in biological systems.

Herein, we report the reactions of bismite (Bi_2O_3) with ammonium tungstate and ammonium molybdate as well as utilising $Bi(NO_3)_3{\cdot}5H_2O$ with ammonium molybdate in order to further access Bi containing polyoxometalates. To demonstrate the utilization of these compounds for biomedical applications, in particular as radiosensitisers, cell viability studies in both human carcinoma and healthy embryonic cells have been carried out.

Results and discussion

Synthetic Procedures

Compounds **1** and **2** were synthesised by reacting Bi_2O_3 with ammonium tungstate or ammonium molybdate in an aqueous solution of 2,5-dimethylbenzenesulfonic acid (Scheme 1). Detailed syntheses (including molar ratios of reactants) of compound **1** and **2** are given in the Experimental Section. In both reactions, ammonium molybdate or ammonium tungstate was added to an aqueous solution of the 2,5-dimethylsulfonic acid, followed by the addition of the Bi_2O_3. The reactions were heated at reflux for 4-5 hours. For the tungsten reaction (Scheme 1, pathway *a*), a cloudy solution was observed which was filtered. The aqueous filtrate was left for slow evaporation and single crystals of $\{(NH_4)_{14}[Bi_2W_{22}O_{76}]{\cdot}14H_2O\}$ (**1**$\cdot 14H_2O$) were isolated (discussed below). Interestingly, the low solubility of the white powder isolated after the reaction with ammonium molybdate meant that the final complex could only be isolated from DMSO. The aqueous filtrate from that reaction (pathway *b*, Scheme 1) simply produced the ammonium salt of the aryl sulfonic acid. In this case, a Bi-Mo ion pair was isolated, rather than a single structure containing both metals, as with structure **1** (discussed in detail below). Commonly, for accessing Bi containing POM, bismuth salts are utilised (e.g., bismuth acetate, bismuth nitrate) with mineral acids (e.g., HCl, HNO_3). Herein, we have shown that the organic sulfonic acid was able to remove bismuth from the generally strong Bi_2O_3 lattice and make it available to form the final POM structures. We are only aware of one report in which Bi_2O_3 has been utilised for the synthesis of $Na_{10}[Bi_2Ni_2W_{20}O_{70}(H_2O)_6]{\cdot}26H_2O$. In this synthetic method, however, 6M HCl was utilised as the acid source.[53]

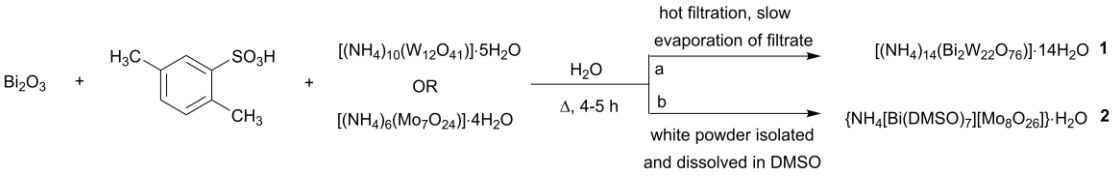

Scheme 1: General synthetic and crystallisation conditions for the isolation of **1** (pathway a) and **2** (pathway b).

We have previously shown that $Bi(NO_3)_3{\cdot}5H_2O$ can react with arylsulfonate salts to produce 2D and 3D coordination networks of polynuclear bismuth oxido/hydroxido sulfonato clusters.[54] Therefore, in an attempt to access a Bi-Mo containing POM, $Bi(NO_3)_3{\cdot}5H_2O$ was used as an alternative bismuth source to the Bi_2O_3. For this reaction, $[(NH_4)_6Mo_7O_{24}]{\cdot}4H_2O$ was added to an aqueous solution of 2,5-dimethylsulfonic acid followed by slow addition of $Bi(NO_3)_3{\cdot}5H_2O$. A white solid was formed during the addition of $Bi(NO_3)_3{\cdot}5H_2O$ and the heterogeneous reaction mixture was stirred overnight. The solution was blue in colour and a white solid was still present. The pale blue solution was kept to slowly evaporate, which resulted in single crystals of $\{[(NH_4)_4(Mo_{36}O_{108}(OH)_4{\cdot}16H_2O)]{\cdot}45H_2O\}$ (**3**$\cdot 45H_2O$) as discussed in detail below. The white solid was isolated, washed with water and ethanol and analysed by IR and EDX. FT-IR indicated that the solid was inorganic and Mo-O asymmetric stretching vibrations and Mo-O-Mo asymmetric stretching vibrations at 938 cm^{-1} and 811 cm^{-1} respecticley[55] were observed. Energy dispersive X-ray spectroscopy (EDX) was used to further confirm the presence of Mo as well as Bi in the isolated white solid (Figure S1). Due to low solubility, solution state

analysis was not achievable and PXRD was not achievable due to the amorphous nature of this solid. Further investigation into this reaction is required to confirm the composition of the white solid.

X-ray crystallography

Single crystals suitable for X-Ray diffraction studies of compound $\{(NH_4)_{14}[Bi_2W_{22}O_{76}]\cdot 14H_2O\}$ (**1**$\cdot 14H_2O$) were obtained by slow evaporation from the aqueous filtrate. The molecular structure of compound **1** contains of two Bi atoms and twenty-two W atoms. These metals are held together by seventy-six O atoms resulting in a caged structure. Compound **1** consists of two identical trilacunary β-$[BiW_9O_{33}]$ pseudo-Keggin type units, which are connected by four WO_2 groups. Formally, the unit can be derived from the Keggin structure by removing one W_3O_{13} fragment. All the W atoms are bonded to six O atoms forming overall octahedron geometry around W centre (Figure 1). Each Bi(III) hetero atom sitting inside the cluster core is bonded to seven O atoms forming hexagonal pyramidal geometry around the Bi centre. Compound **1** is isostructural to previously published structure $Na_{12}[Bi_2W_{22}O_{74}(OH)_2]\cdot 44H_2O$.[56]

Energy dispersive X-ray spectroscopy studies were carried out on crystalline samples of compounds **1** - **3** to confirm the presence of Bi, W and Mo in each sample (Figure S2-S4). Powdered X-ray diffraction (PXRD) studies were conducted to confirm the bulk crystalline material is same as the structure obtained from the single crystal X-ray diffraction. Compound **1** and **2** produced a matching powder pattern when compared with the calculated powder pattern deduced from the single crystal X-ray data (Figures S5 and S6). However, compound **3** did not produce a matching PXRD due to presence of few polymorphs of the same complex (Figure S7). These polymorphs have been identified and their single crystal details are given in Table S1 (ESI).

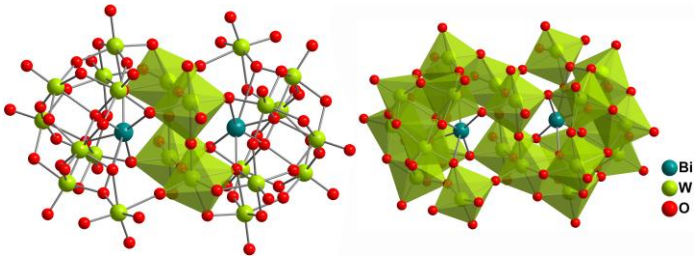

Figure 1. Ball and stick representation of the molecular structure of compound $[NH_4]_{14}[Bi_2W_{22}O_{76}]$ (**1**) (left). Octahedron geometry around W centres represented in green colour polyhedrons (right).

Upon crystallisation from DMSO, the product from the reaction of Bi_2O_3 with the sulfonic acid and ammonium molybdate, was isolated as an ion pair: $\{NH_4[Bi(DMSO)_7][Mo_8O_{26}]\}\cdot H_2O$ (**2**), Figure 2. The structure consists of two $[Mo_8O_{26}]^{2-}$ groups and a DMSO coordinated Bi^{3+} centre, as well as an NH_4^+ ion.

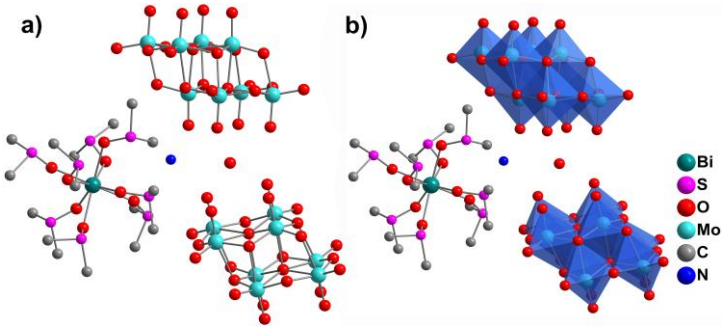

Figure 2. Ball and stick representation of molecular structure of compound $\{NH_4[Bi(DMSO)_7][Mo_8O_{26}]\cdot H_2O\}$ (**2**$\cdot H_2O$) (a). Octahedron geometry around Mo centres are represented by the blue polyhedrons (b).

In compound **2** all the Mo centres are bound to six oxygen atoms making an overall octahedral geometry around the metal centre. This ion pair is not a common motif, however one similar bismuth containing ion pair structure has been reported, $\{[Na(BiEDTA\cdot 2H_2O)_3][PMo_{12}O_{40}]\}\cdot 4H_2O$ (H_4EDTA = ethylenediamintetraacetic acid).[57]

Single crystals of compound **3** {$[(NH_4)_4(Mo_{36}O_{108}(OH)_4{\cdot}16H_2O)]{\cdot}45H_2O$} (**3**$\cdot 45H_2O$) suitable for X-ray diffraction were obtained by slow evaporation from the aqueous filtrate. Compound **3** consists of thirty-six Mo(VI) atoms directly bonded to oxygen. The majority of Mo(VI) atoms are in an octahedral geometry which is highlighted by the dark blue polyhedrons in Figure 3b. There are four Mo(VI) centres, each bound to seven oxygen atoms, forming a pentagonal bipyramidal coordination geometry around Mo(VI) centres (Figure 3, pink polyhedrons). The cluster core of {$[(NH_4)_4(Mo_{36}O_{108}(OH)_4{\cdot}16H_2O)]{\cdot}45H_2O$} is made up of a centrosymmetric assembly of two Mo18 subunits. In this case, the acidification of $[(NH_4)_6Mo_7O_{24}]{\cdot}4H_2O$ with the aryl sulfonic acid favoured formation of the Mo_{36} cluster over a mixed Bi-Mo cluster. This is not unexpected as it is well known that the acidification of an aqueous solution of molybdate under ambient conditions yields the {Mo_{36}} type cluster,[58,59] e.g., $[Mo_{36}O_{108}(OH)_4{\cdot}16H_2O]^{4-}$ which crystallised readily from the aqueous solution.[60]

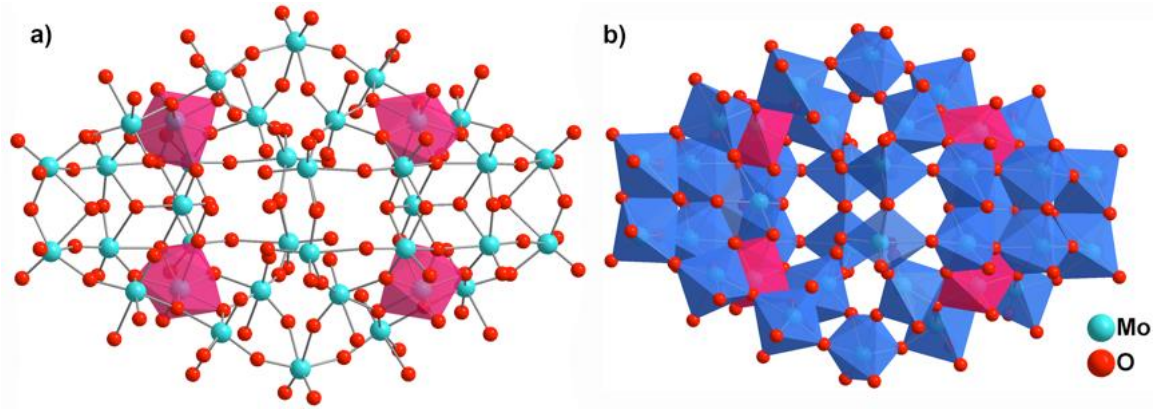

Figure 3. (a) Ball and stick representation of molecular structure of compound {$[(NH_4)_4(Mo_{36}O_{108}(OH)_4{\cdot}16H_2O)]{\cdot}45H_2O$} (**3**$\cdot 45H_2O$). (b) Pentagonal bipyramidal coordination geometry around Mo centre is represented in pink colour polyhedron and octahedron geometry in blue colour polyhedrons.

Mass spectroscopic analysis

Electrospray-ionization mass spectrometry (ESI-MS) has proven to be a valuable analytical technique, for the further characterisation of POMs and a way to underscore their behaviour in solution.[61] Mass spectrometry was carried out on a freshly prepared water solution of {$(NH_4)_{14}[Bi_2W_{22}O_{76}]{\cdot}14H_2O$} (**1**$\cdot 14H_2O$). ESI-MS suggests that in solution, compound **1** breaks apart and each of these 'halves' form smaller fragments upon ionisation in the mass spectrometer. Figure 4 shows the ESI-MS of compound **1** (negative ion mode). The major peaks are a series of envelopes representing the singly charged $[BiW_xO_y]^-$ anions. The mass difference of the main envelopes can be attributed to the mass of a WO_3 group.

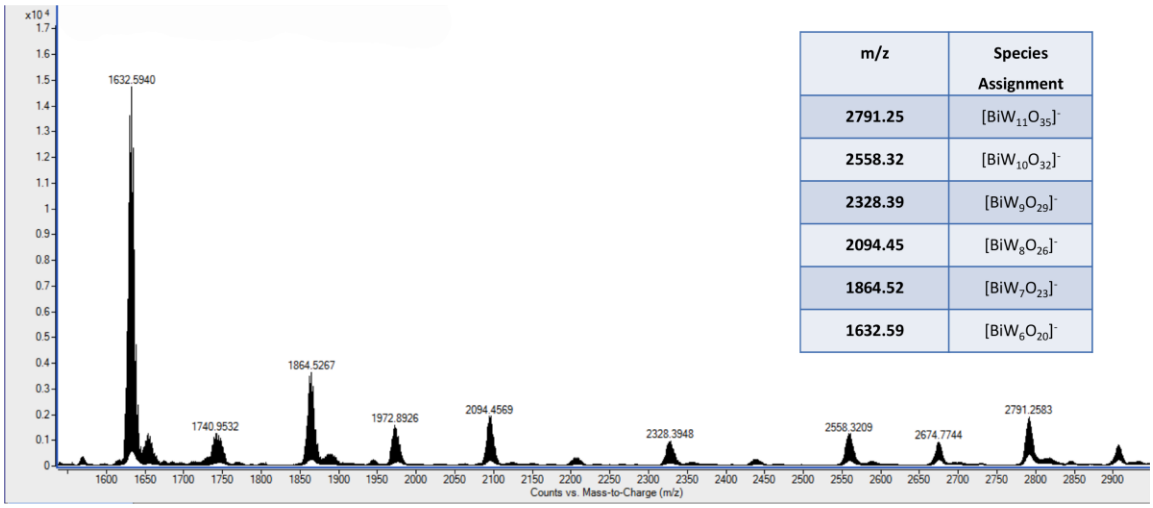

m/z	Species Assignment
2791.25	$[BiW_{11}O_{35}]^-$
2558.32	$[BiW_{10}O_{32}]^-$
2328.39	$[BiW_9O_{29}]^-$
2094.45	$[BiW_8O_{26}]^-$
1864.52	$[BiW_7O_{23}]^-$
1632.59	$[BiW_6O_{20}]^-$

Figure 4. Negative ion ESI-MS spectrum of compound **1** in water showing a series of species derived from $[BiW_{10}O_{32}]^-$.

The m/z peak at 2791.25 can be assigned to the polyanion assembly $[BiW_{11}O_{35}]^-$. Then it loses one WO_3 group at a time until it gives the most abundant peak (in higher mass region) at m/z = 1632.59 $[BiW_6O_{20}]^-$. This process is evidenced by the m/z peaks obtained at; 2558.32 $[BiW_{10}O_{32}]^-$, 2328.39 $[BiW_9O_{29}]^-$, 2094.45 $[BiW_8O_{26}]^-$ and 1864.52 $[BiW_7O_{23}]^-$ respectively (Figure 4). For each major signal shown in Figure 4, the corresponding experimental and predicted isotope patterns are shown in the Supporting Information, Figures S8-S19. Whilst attempts were made to collect ESI-MS data for $\{NH_4[Bi(DMSO)_7][Mo_{16}O_{48}]\cdot H_2O\}$ (**2**$\cdot H_2O$), the poor aqueous solubility of the compound precluded it from suitable analysis. Attempts were made to analyse compound **3** using ESI-MS however even though **3** is soluble in hot water, it was not able to be ionised and therefore no useful MS data was obtained.

Raman Spectroscopy

Compounds **1-3** were further characterised using Raman spectroscopy. For $\{(NH_4)_{14}[Bi_2W_{22}O_{76}]\cdot 14H_2O\}$ (**1**$\cdot 14H_2O$), characteristic symmetric W=O and W-O-W stretching vibrations were observed at 971(s) ν$_s$ W=O, 892 (m) and asymmetric stretching vibration of W-O-W was observed at 779 cm^{-1} (Figure S20). These vibrational values agree with the literature reported values of similar complexes.[55] $\{NH_4[Bi(DMSO)_7][Mo_8O_{26}]\cdot H_2O\}$ (**2**) and $\{[(NH_4)_4(Mo_{36}O_{108}(OH)_4\cdot 16H_2O)]\cdot 45H_2O$ (**3**$\cdot 45H_2O$) show the characteristic symmetric and asymmetric stretching vibration bands of Mo-O at 965(s) and 959(s) cm^{-1} (Figures S21 and S22). These signals are in good agreement with previously published MoO_3 complexes.[55]

Thermogravimetric analysis (TGA)

TGA was conducted on **1** - **3** (Figures S23-S25, Supporting Information). Clusters **1** and **3** gave mass losses of 9 % and 11 % respectively. This mass loss can be attributed to the loss of lattice and coordinated water molecules, leaving the remaining stable metal oxide framework. Compound **2** shows a greater mass loss of 38 %, due to the loss of a coordinated DMSO molecules at the Bi(III) centre (Figure 2).

Proliferation and cytotoxicity studies

Ideally, agents to be applied as radiosensitisers should be *per se* non-toxic. They should only develop their efficacy after irradiation with photons or protons and thus improve conventional radiotherapy.[39,62] In this context, we have studied the *in vitro* behaviour of two cluster compounds in both a cancer and healthy cell line. Hence, clusters **1** and **3** were tested in A431 (human squamous carcinoma) and HEK293 (human embryonic kidney) cells utilising the MTS (*[3-(4,5-dimethylthiazol-2-yl)-5-(3-carboxymethoxyphenyl)-2-(4-sulfophenyl)-2H-tetrazolium]*), CyQuant and LDH (lactate dehydrogenase) assays to investigate the biologic potential of the clusters (**2** did not undergo testing due to limited aqueous solubility). The MTS assay determines the number of viable cells. The CyQuant proliferation assay quantifies DNA content. The cytotoxicity assay however investigates the amount of released lactate dehydrogenase (LDH) which only occurs from damaged cells. Cells undergoing necrosis or apoptosis release LDH and the enhanced activity can be quantified. All assays were conducted in each cell line treated with different concentrations of **1** and **3** ranging from 0 up to 0.75 mg/mL (15 to 121 µM) in 1% (v/v) DMSO in water. Adding amounts higher than 0.75 mg/mL of clusters to the cell culture medium resulted in the formation of precipitates.

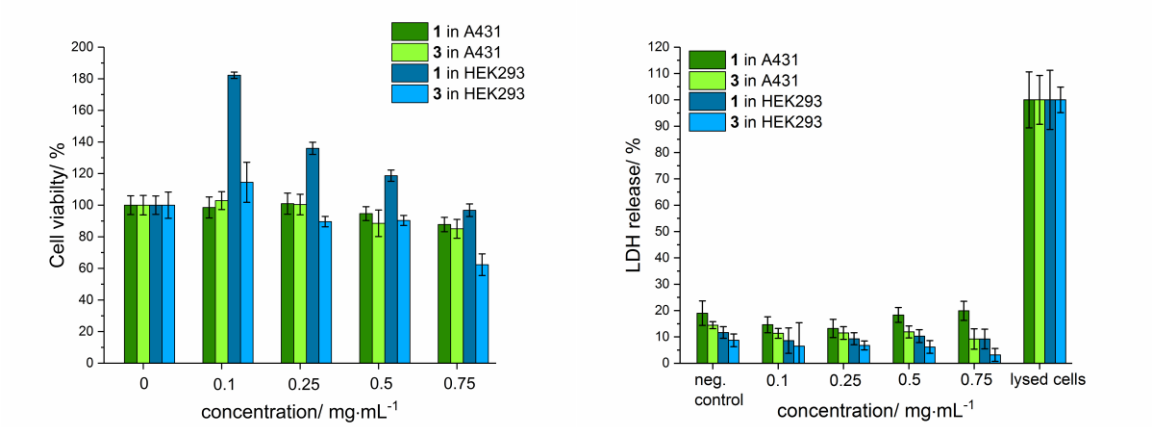

Figure 5. MTS (left) and LDH (right) assay of **1** and **3** using different concentrations (0, 0.1, 0.25, 0.5 and 0.75 mg/mL) in A431 (green bars) and HEK293 (blue bars) cell line after 24 h incubation. The percentage of cell viability is expressed relative to untreated control cells.

The MTS assay revealed that $\{(NH_4)_{14}[Bi_2W_{22}O_{76}]\cdot 14H_2O\}$ (**1**·$14H_2O$) and $\{[(NH_4)_4(Mo_{36}O_{108}(OH)_4\cdot 16H_2O)]\cdot 45H_2O\}$ (**3**·$45H_2O$) had no significant influence on the viability of A431 cells after 24 hours within the investigated concentration range (see Figure 5). Interestingly, when **1** (up to 0.5 mg/mL or 81 µM) was incubated in HEK 293, the cell viability was boosted. A significant decrease of cell viability was observed only for compound **3** using 0.75 mg/mL (117 µM) in HEK293 cell line. The results of the CyQuant assay are shown in Figure S26. No decrease on the cellular DNA content could be detected for compound **1** and **3** in the tumour cell line. In addition, no cytotoxic effect was observed for compound **1** or **3** in the respective cell lines using the LDH assay. As positive control, we used lysed cells. Lysed cells suffer from plasma membrane damages and produce the cytoplasmic enzyme LDH. Damaged cells therefore showed 100% of LDH release. In comparison, the negative control (without addition of compound **1** an **3**)

revealed similar values as the cells treated with the compounds. This indicates that the compounds did not affect the cells.

While our results show that these clusters may be suitable for use as radiosensitisers. This must be demonstrated by further investigation under the influence of ionising radiation.

Conclusions

We have discovered a method to utilise naturally occurring bismite (Bi_2O_3) to form bismuth containing POMs in the presence of $(NH_4)_{10}W_{12}O_{41}\cdot 5H_2O$ and an arylsulfonic acid. The sulfonic acid helps to break down the Bi_2O_3 lattice and make bismuth atoms available for the formation of bismuth and tungsten containing POM $\{(NH_4)_{14}[Bi_2W_{22}O_{76}]\cdot 14H_2O\}$ (**1**$\cdot 14H_2O$). However, in the presence of $(NH_4)_6Mo_7O_{24}\cdot 4H_2O$, a bismuth containing ion par associated with a molybdenum-POM resulted, $\{NH_4[Bi(DMSO)_7][Mo_8O_{26}]\cdot H_2O\}$ (**2**$\cdot H_2O$). When $Bi(NO_3)_3\cdot 5H_2O$ was used as bismuth source the expected mixed metal POM was not observed and instead a homometallic POM, $\{[(NH_4)_4(Mo_{36}O_{108}(OH)_4\cdot 16H_2O)]\cdot 45H_2O\}$ (**3**$\cdot 45H_2O$) was isolated. *In vitro* studies of **1** and **3** using human cancer and healthy cells revealed minimal cytotoxicity. This makes these clusters very attractive as potential radiosensitisers in oncology.

Experimental

Synthesis procedures

Synthesis of $\{(NH_4)_{14}[Bi_2W_{22}O_{76}]\cdot 14H_2O\}$ (**1**$\cdot 14H_2O$)

Solid powder of $(NH_4)_{10}W_{12}O_{41}\cdot 5H_2O$ (0.2 mmol) was added to the aqueous solution (100 ml) of 2,5-dimethylsulfonic acid (0.6 mmol) followed by Bi_2O_3 (O.1 mmol). Heterogeneous mixture was refluxed for 4 hrs. The resulted cloudy solution was filtered hot and left for crystallisation. Yield: 0.492 g (81%). Anal. Calcd for $Bi_2H_{84}N_{14}O_{90}W_{22}$: H, 1.37; N, 3.17. Found: H, 1.34; N, 3.43. Raman (cm^{-1}): ν = 3106w, 1677w, 1427w, 971s (W=O), 916m, 892m (W=O), 847m, 779m (W-O-W), 721w, 602m, 532w, 462w, 409w, 337w, 220m, 158m, 106w. ESI-MS in water (negative): m/z =1632.59 $[BiW_6O_{20}]^-$, m/z =1864.52 $[BiW_7O_{35}]^-$, m/z =2094.45 $[BiW_8O_{26}]^-$, m/z =2328.39 $[BiW_9O_{29}]^-$, m/z =2558.32 $[BiW_{10}O_{32}]$ and m/z =2791.25 $[BiW_{11}O_{35}]^-$.

Synthesis of $\{NH_4[Bi(DMSO)_7][Mo_8O_{26}]\cdot H_2O\}$ (**2**$\cdot H_2O$)

Solid powder of $(NH_4)_6Mo_7O_{24}\cdot 4H_2O$ (0.32 mmol) was added to the aqueous solution of 2,5-dimethylsulfonic acid (0.6 mmol) followed by Bi_2O_3 (0.1 mmol). Heterogeneous mixture was refluxed for 4 hrs. The resulted white solid was washed with water, dissolved in hot DMSO and left for crystallisation after 2 months white colour crystals of $\{NH_4[Bi(DMSO)_7][Mo_8O_{26}]\}$ were obtained. Yield: 0.321 g (64%). Anal. Calcd for: $C_{16}H_{84}BiMo_8NO_{40}S_{13}$: C, 9.36; H, 2.65; N, 0.68. Found: C, 9.31; H, 2.52; N, 0.42. Formula deduced from the elemental analysis results $\{NH_4[Bi(DMSO)_7][Mo_8O_{26}]\cdot H_2O\cdot DMSO\}$. Raman ($cm^{-1}$): ν = 3010s, 2918s, 1414m, 1022w, 992m, 965s (Mo-O), 945s, 923w, 909m, 837m, 719m, 684s, 519w, 364w, 307m, 247m, 226m, 204m.

Synthesis of $\{[(NH_4)_4(Mo_{36}O_{108}(OH)_4\cdot 16H_2O)]\cdot 45H_2O\}$ (**3**$\cdot 45H_2O$).

Solid powder of $(NH_4)_6Mo_7O_{24}\cdot 4H_2O$ (0.32 mmol) was added to the aqueous solution of 2,5-dimethylsulfonic acid (0.3 mmol) followed by slow addition of $Bi(NO_3)_3\cdot 5H_2O$ (0.1 mmol). White colour solid was formed

during the addition of $Bi(NO_3)_3 \cdot 5H_2O$. The heterogeneous reaction mixture was refluxed for 4-5 hours. The resulted pale blue solution and the white colour solid was isolated. Upon slow evaporation of pale blue solution white colour crystals of $\{[(NH_4)_4(Mo_{36}O_{108}(OH)_4 \cdot 16H_2O)] \cdot 45H_2O\}$ were obtained. Yield: 0.173 g (34%). Raman (cm^{-1}): ν = 3142w, 993w, 959s (Mo-O), 892s, 848w, 616w, 539w, 503w, 452m, 367w, 234m, 120w.

Cell culture conditions

The human A431 (skin epidermoid carcinoma) and HEK 293 (human embryonic kidney) cell lines were purchased from CLS (Cell Lines Service GmbH, Eppelheim, Germany) and DSMZ (Leibniz Institute DSMZ-German Collection of Microorganisms and Cell Cultures). The cell lines were cultured in Dulbecco's modified Eagle's medium (DMEM, Biochrom) supplemented with 10% standardised fetal bovine serum (FBS, Biochrom) and 1:100 (v/v) penicillin/ streptomycin (Biochrom) solution. Cells were incubated in 75 cm^2 culture cell flasks at 37 °C in a humidified atmosphere enriched with 5% CO_2.

Proliferation and cytotoxicity studies

The proliferation (MTS [3-(4,5-dimethyl-2-yl)-5-(3-carboxymethoxyphenyl)-2-(4-sulfophenyl)-2H-tetrazolium] and CyQuant) and cytotoxicity (LDH, lactate dehydrogenase) studies were conducted in A431 and HEK293 cell lines. 50 µL cell suspension in culture medium were plated in each well. Cells were seeded with 6000 cells/well in transparent flat bottom 96-well plates (Cellstar, Greiner Bio-One GmbH, Frickenhausen, Germany). Stock solutions of **1** and **3** with 7.5mg/mL were prepared in 10% (v/v) aqueous DMSO (Hybri-Max, Sigma-Aldrich). After 24 h, 50 µL of **1** and **3** with varying concentrations (0/ 0.1/ 0.25/ 0.5/ 0.75 mg/mL, final concentration of 1% (v/v) aqueous DMSO) were added to each well. The 96-well plates were incubated at 37 °C in a humidified atmosphere enriched with 5% CO_2 for 1, 4, 24 and 48 h. Controls contain 1 % (v/v) DMSO and were treated in the same way without adding compound **1** or **3** to the respective cell line. For determination of the proliferation and cytotoxicity, commercially available kits as MTS (CellTiter 96® AQ_{ueous} One Solution Cell Proliferation Assay, Promega), CyQuant (CyQUANT Proliferation Assay, Invitrogen, ThermoFisher) and LDH (CytoScan LDH Cytotoxcicty Assay, G-Bioscience) were used according to the manufactures instructions. In brief, MTS and LDH are colorimetric assays to determine either the number of living cells or the amount of released LDH enzyme. The CyQuant assay is a fluorescence-based method where the dye binds to the DNA to determine the cellular DNA content. All cells are quantified by either their corresponding fluorescence (λ_{ex} = 508/λ_{em} = 535nm, CyQUANT) properties or the formation of formazan ($A_{\lambda max}$ = 492 nm, MTS and LDH) using microplate readers from ThermoFisher Scientific (VarioskanFlash) and Tecan (Sunrise). All experiments were performed in triplicates and calculations were performed using excel and Origin2017G (OriginLab Corporation, Northampton, USA).

Acknowledgements

The authors thank Monash University, the Australian Research Council (DP170103624), the Helmholtz Initiative and Networking Fund, and HZDR (NanoTracking, project ID: VH-VI-421) for financial support. We thank Dr Craig Forsyth (Monash) for assistance with X-ray crystallography, Dr George Khairallah (Monash) for mass spectrometry, and Utta Herzog (HZDR) for excellent technical assistance during cell experiments. M.K.

was supported by a Marie Curie International Outgoing Fellowship from the European Union's Seventh Framework Programme for research, technological development and demonstration under grant agreement no. 627113.

References

1 J. T. Rhule, C. L. Hill, D. a. Judd and R. F. Schinazi, *Chem. Rev*., 1998, **98**, 327–358.

2 S.-S. Wang and G.-Y. Yang, *Chem. Rev.,* 2015, **115**, 4893–4962.

3 L. Vilà-Nadal and L. Cronin, *Nat. Rev. Mater*. DOI:10.1038/natrevmats.2017.54.

4 D. Mendoza-Espinosa and T. A. Hanna, *Inorg. Chem*., 2009, **48**, 7452–7456.

5 S. T. Zheng and G. Y. Yang, *Chem. Soc. Rev*., 2012, **41**, 7623–7646.

6 C. L. Hill and C. M. Prosser-McCartha, *Coord. Chem. Rev*., 1995, **143**, 407–455.

7 P. Gouzerh and A. Proust, *Chem. Rev.,* 1998, **98**, 77–112.

8 U. Kortz, A. Müller, J. van Slageren, J. Schnack, N. S. Dalal and M. Dressel, *Coord. Chem. Rev.*, 2009, **253**, 2315–2327.

9 O. Oms, A. Dolbecq and P. Mialane, *Chem. Soc. Rev.*, 2012, **41**, 7497–7536.

10 Y. Yong, C. Zhang, Z. Gu, J. Du, Z. Guo, X. Dong, J. Xie, G. Zhang, X. Liu and Y. Zhao, *ACS Nano*, 2017, **11**, 7164–7176.

11 D. Ni, D. Jiang, C. J. Kutyreff, J. Lai, Y. Yan, T. E. Barnhart, B. Yu, H. J. Im, L. Kang, S. Y. Cho, Z. Liu, P. Huang, J. W. Engle and W. Cai, *Nat. Commun.,* DOI:10.1038/s41467-018-07890-8.

12 J. T. Rhule, C. L. Hill, D. A. Judd and R. F. Schinazi, *Chem. Rev.,* 2002, **98**, 327–358.

13 M. Barsukova-Stuckart, L. F. Piedra-Garza, B. Gautam, G. Alfaro-Espinoza, N. V. Izarova, A. Banerjee, B. S. Bassil, M. S. Ullrich, H. J. Breunig, C. Silvestru and U. Kortz, *Inorg. Chem*., 2012, **51**, 12015–12022.

14 K. D. Mjos and C. Orvig, *Chem. Rev.*, 2014, **114**, 4540–4563.

15 P. Yang, B. S. Bassil, Z. Lin, A. Haider, G. Alfaro-Espinoza, M. S. Ullrich, C. Silvestru and U. Kortz, *Chem Eur. J.,* 2015, **21**, 15600–15606.

16 P. Yang, Z. Lin, B. S. Bassil, G. Alfaro-Espinoza, M. S. Ullrich, M. X. Li, C. Silvestru and U. Kortz, *Inorg. Chem.,* 2016, **55**, 3718–3720.

17 P. Yang, Z. Lin, G. Alfaro-Espinoza, M. S. Ullrich, C. I. Raţ, C. Silvestru and U. Kortz, *Inorg. Chem.,* 2016, **55**, 251–258.

18 J. Wang, Y. Liu, K. Xu, Y. Qi, J. Zhong, K. Zhang, J. Li, E. Wang, Z. Wu and Z. Kang, *ACS Appl. Mater*. *Interfaces*, 2014, **6**, 9785–9789.

19 E. De Clercq, *Med. Res. Rev.*, 2002, **22**, 531–565.

20 M. Fukuma, Y. Seto and T. Yamase, *Antiviral Res.,* 1991, **16**, 327–339.

21 A. Bijelic, M. Aureliano and A. Rompel, *Chem. Commun.*, 2018, **54**, 1153–1169.

22 X. Gao, J. Gu, X. Yuan, D. Li, L. Zhang and Y.-G. Chen, *Bioinorg. Chem. Appl*., 2018, **2018**, 1–6.

23 L. Grama, A. Man, D. L. Muntean, S. A. G. Florea, F. Boda and A. Curticăpean, *Rev. Rom. Med. Lab.*, 2014, **22**, 111–118.

24 H. Stephan, M. Kubeil, F. Emmerling and C. E. Müller, *Eur. J. Inorg. Chem.*, 2013, **2013**, 1585–1594.

25 B. Hasenknopf, Front. *Biosci.,* 2005, **10**, 275.

26 E. De Clercq, *Rev. Med. Virol.*, 2000, **10**, 255–277.

27 T. Yamase, *Biomedical Inorganic Polymers*, 2013, 54, 65-116.

28 M. Aureliano and D. C. Crans, *J. Inorg. Biochem*., 2009, **103**, 536–546.

29 A. Bijelic, M. Aureliano and A. Rompel, *Angew. Chemie - Int. Ed.*, 2018, 2980–2999.

30 S. Y. Lee, S. Sarkar, S. Bhattarai, V. Namasivayam, S. De Jonghe, H. Stephan, P. Herdewijn, A. El-Tayeb and C. E. Müller, *Front. Pharmacol.,* 2017, **8**, 1–7.

31 S. Y. Lee, A. Fiene, W. Li, T. Hanck, K. A. Brylev, V. E. Fedorov, J. Lecka, A. Haider, H. J. Pietzsch, H. Zimmermann, J. Sévigny, U. Kortz, H. Stephan and C. E. Müller, *Biochem. Pharmacol.*, 2015, **93**, 171–181.

32 H. Stephan, M. Kubeil, F. Emmerling and C. E. Müller, *Eur. J. Inorg. Chem*., 2013, 1585–1594.

33 F. F. Bamoharram, M. M. Heravi, J. Ebrahimi, A. Ahmadpour And M. Zebarjad, *Chinese J. Catal*., 2011, **32**, 782–788.

34 F. F. Bamoharram, M. Roshani, M. H. Alizadeh, H. Razavi and M. Moghayadi, *J. Braz. Chem. Soc.*, 2006, **17**, 505–509.

35 F. F. Bamoharram, M. M. Heravi, M. Roshani, M. Jahangir and A. Gharib, *Appl. Catal. A Gen*., 2006, **302**, 42–47.

36 R. Weast, Handbook of chemistry and physics: a ready-reference book of chemical and physical data, CRC Press, Cleveland, Ohio, 58th edn., 1977.

37 S. B. Yu and A. D. Watson, *Chem. Rev.,* 1999, **99**, 2353–2377.

38 A. Detappe, E. Thomas, M. W. Tibbitt, S. Kunjachan, O. Zavidij, N. Parnandi, E. Reznichenko, F. Lux, O. Tillement and R. Berbeco, *Nano Lett.*, 2017, **17**, 1733–1740.

39 J. Xie, L. Gong, S. Zhu, Y. Yong, Z. Gu and Y. Zhao, *Adv. Mater.*, 2019, **31**, 1–25.

40 K. S. Egorova and V. P. Ananikov, *Organometallics,* 2017, **36**, 4071–4090.

41 G. F. Nordberg, B. A. Fowler and M. Nordberg, Eds., Handbook on the Toxicology of Metals, Academic Press, Stockholm, 4th edn., 2015.

42 R. Zhou, H. Wang, Y. Yang, C. Zhang, X. Dong, J. Du, L. Yan, G. Zhang, Z. Gu and Y. Zhao, *Biomaterials,* 2019, **189**, 11–22.

43 L. Wang, B. Bin Zhou, K. Yu, Z. H. Su, S. Gao, L. L. Chu, J. R. Liu and G. Y. Yang, *Inorg. Chem.*, 2013, **52**, 5119–5127.

44 Z. Wang and Y. Sun, *Transl. Oncol.,* 2010, **3**, 1–12.

45 S. G. Mitchell, S. Khanra, H. N. Miras, T. Boyd, D.-L. Long and L. Cronin, *Chem. Commun*., 2009, 2712–2714.

46 A. H. Ismail, B. S. Bassil, I. Römer, N. C. Redeker and U. Kortz, *Zeitschrift fur Naturforsch. - Sect. B J. Chem. Sci.*, 2010, **65**, 383–389.

47 T. Hanaya, K. Suzuki, R. Sato, K. Yamaguchi and N. Mizuno, *Dalt. Trans.*, 2017, **46**, 7384–7387.

48 A. Pathak, V. L. Blair, R. L. Ferrero, M. Mehring and P. C. Andrews, *Chem. Commun*., 2014, **50**, 15232–15234.

49 J. H. Thurston, D. C. Swenson and L. Messerle, *Chem. Commun.,* 2005, **4**, 4228–4230.

50 M. Mehring, Coord. Chem. Rev., 2007, **251**, 974–1006.

51 L. Miersch, T. Rüffer, D. Schaarschmidt, H. Lang, R. W. Troff, C. A. Schalley and M. Mehring, *Eur. J. Inorg. Chem.*, 2013, **2013**, 1427–1433.

52 D. C. Senevirathna, V. L. Blair, M. V. Werrett and P. C. Andrews, *Inorg. Chem.,* 2016, **55**, 11426–11433.

53 D. Rodewald and Y. Jeannin, *Comptes Rendus l'Académie des Sci. - Ser. IIC - Chem*., 2002, **1**, 175–181.

54 D. C. Senevirathna, M. V Werrett, V. L. Blair, M. Mehring and P. C. Andrews, *Chem. Eur. J*., 2018, **24**, 6722–6726.

55 R. Thouvenot, M. Fournier, R. Franck and C. Rocchiccioli-Deltcheff, *Inorg. Chem*., 1984, **23**, 598–605.

56 I. Loose, E. Droste, M. Bösing, H. Pohlmann, M. H. Dickman, C. Rosu, M. T. Pope and B. Krebs, *Inorg. Chem.,* 1999, **38**, 2688–2694.

57 C. L. Teng, H. X. Xiao, Q. Cai, J. T. Tang, T. J. Cai and Q. Deng, *J. Coord. Chem.*, 2016, **69**, 2148–2163.

58 A. Muller, E. Krickemeyer, S. Dillinger, H. Bogge, W. Plass, A. Proust, L. Dloczik, C. Menke, J. Meyer and R. Rohlfing, *Zeitschrift f*[illegible]*Anorg. und Allg. Chemie*, 1994, **620**, 599–619.

59 B. Krebs and I. Paulat-Böschen, *Acta Crystallogr. Sect. B Struct. Crystallogr. Cryst. Chem*., 1982, **38**, 1710–1718.

60 D. L. Long, C. Streb, P. Kögerler and L. Cronin, *J. Clust. Sci.*, 2006, **17**, 257–266.

61 K.-Y. Wang, B. S. Bassil, Z.-G. Lin, A. Haider, J. Cao, H. Stephan, K. Viehweger and U. Kortz, *Dalt. Trans.,* 2014, **43**, 16143–16146.

62 L. A. Kunz-Schughart, A. Dubrovska, C. Peitzsch, A. Ewe, A. Aigner, S. Schellenburg, M. H. Muders, S. Hampel, G. Cirillo, F. Iemma, R. Tietze, C. Alexiou, H. Stephan, K. Zarschler, O. Vittorio, M. Kavallaris, W. J. Parak, L. Mädler and S. Pokhrel, *Biomaterials,* 2017, **120**, 155–184.